

1 **Analysis of historical selection in winter wheat**

2 Chin Jian Yang*

3 Olufunmilayo Ladejobi†

4 Richard Mott†

5 Wayne Powell*

6 Ian Mackay*‡

7 *Scotland's Rural College (SRUC), Kings Buildings, West Mains Road, Edinburgh, EH9 3JG,
8 UK.

9 †Department of Genetics, Evolution & Environment, University College London, London, WC1E
10 6BT

11 ‡IMPlant Consultancy Ltd., Chelmsford, UK.

12 Corresponding author: Ian Mackay, ian.mackay@sruc.ac.uk

13

14 **Abstract**

15 Winter wheat is a major crop with a rich selection history in the modern era of crop breeding.
16 Genetic gains across economically important traits like yield have been well characterized and
17 are the major force driving its production. Winter wheat is also an excellent model for analyzing
18 historical genetic selection. As a proof of concept, we analyze two major collections of winter
19 wheat varieties that were bred in western Europe from 1916 to 2010, namely the Triticeae
20 Genome (TG) and WAGTAIL panels, which include 333 and 403 varieties respectively. We
21 develop and apply a selection mapping approach, Regression of Alleles on Years (RALLY), in
22 these panels, as well as in simulated populations. RALLY maps loci under sustained historical
23 selection by using a simple logistic model to regress allele counts on years of variety release.
24 To control for drift-induced allele frequency change, we develop a hybrid approach of genomic
25 control and delta control. Within the TG panel, we identify 22 significant RALLY quantitative
26 selection loci (QSLs) and estimate the local heritabilities for 12 traits across these QSLs. By
27 correlating predicted marker effects with RALLY regression estimates, we show that alleles
28 whose frequencies have increased over time are heavily biased towards conferring positive
29 yield effect, but negative effects in flowering time, lodging, plant height and grain protein
30 content. Altogether, our results (1) demonstrate the use of RALLY to identify selected genomic
31 regions while controlling for drift, and (2) reveal key patterns in the historical selection in winter
32 wheat and guide its future breeding.

33

34 **Key Message**

35 Modelling of the distribution of allele frequency over year of variety release identifies major loci
36 involved in historical breeding of winter wheat.

37 **Keywords**

38 RALLY, allele regression, genomic control, selection mapping, genetic gain

39

40 **Introduction**

41 Modern agriculture benefits from long standing breeding effort in creating new and
42 improved crop varieties over time. Genetic gain is often used as a measure of the success in
43 breeding for trait improvement. For example, in wheat, the genetic gains in yield and other
44 agriculturally valuable traits have been well quantified (Mackay et al. 2011, Tadesse et al. 2019
45 and Shorinola et al. 2021). The introduction of genomic selection (GS) (Meuwissen et al. 2001)
46 in breeding program further shortens breeding cycles, improves selection accuracy and
47 intensity, and accelerates genetic gain (Voss-Fels et al. 2019). Lastly, genetic gain is further
48 increased by the rise of knowledge exchange between plant and animal breeding through GS
49 (Hickey et al. 2017).

50 In recent years, there has been a growing interest in mapping quantitative selection loci
51 (QSLs) that are associated with genetic gain independently of any phenotype. The mapping
52 approach typically involves correlating continuous variables, such as year of variety release and
53 geographical parameters, to genomic markers in a historical variety dataset. Conceptually, it is
54 similar to selection mapping which tests for selection signatures among genomic markers using
55 population genetic models (Johnsson 2018). This approach has been variously named as Birth
56 Date Selection Mapping (Decker et al. 2012), Generation Proxy Selection Mapping (Rowan et
57 al. 2021) and EnvGWAS (Li et al. 2020, Sharma et al. 2021). Here, we will refer to it as
58 EnvGWAS because the underlying mixed linear model is no different from a conventional
59 genome-wide association study (GWAS).

60 Related to EnvGWAS, EigenGWAS uses eigenvectors (principal components) as the
61 dependent variable in a mixed linear model (Li et al. 2020, Sharma et al. 2021). The
62 EigenGWAS approach may yield similar results to EnvGWAS if the dependent variables in
63 EnvGWAS are correlated strongly with any eigenvector. Otherwise, EigenGWAS may identify
64 additional QSLs where it incorporates variables that have not been quantified directly. A key
65 confounding factor for determining whether a locus has been under sustained historical
66 selection or drift is that varieties are linked by a complex historical pedigree and unequal
67 relatedness. By correcting for population structure using a mixed linear model (Yu et al. 2006),
68 year effects and principal components that are associated with drift can be controlled in
69 EnvGWAS and EigenGWAS respectively.

70 Here, we introduce a new application of an old method by modelling allele frequency
71 change over years in a historical variety dataset. This method, termed Regression of Alleles on
72 Years (RALLY), fits a logistic regression to model the allele count as a dependent variable and
73 the year of variety release as an independent variable. A logistic model is commonly used in
74 case-control studies where the dependent variables are binary traits of whether an individual is
75 diseased and the independent variables are test factors (Prentice and Pyke 1979). A logistic
76 model is appropriate because changes in allele frequencies are small when the starting
77 frequencies are near the extrema, and large when they are intermediate. In addition, the model
78 is bounded asymptotically by 0 and 1. The dependent and independent variables are switched
79 between RALLY and EnvGWAS. Instead of estimating the mean of years of release for each
80 allele in EnvGWAS, RALLY estimates the mean of allele counts for each year, which is
81 equivalent to the allele frequency for a given year. Recently, Looseley et al. (2020) applied a
82 similar approach to RALLY on significant GWAS markers in a historical barley variety dataset.
83 RALLY is a genome-wide approach that employs parametric control (PC) as a correction to drift-
84 induced allele frequency change. PC is a novel hybrid approach of genomic control (GC) (Devlin

85 and Roeder 1999) and delta control (DC) (Gorroochurn et al. 2006), which are two common
86 control approaches against population structure in human GWAS studies without the need for
87 mixed linear model.

88 Our analyses in the simulated and historical variety datasets demonstrate the usefulness
89 of RALLY in mapping QSLs. We begin the evaluation of RALLY in simulated populations where
90 the truth is known, both with and without selection, to quantify RALLY detection power and limit.
91 We use the simulations to calibrate PC, which is then applied to the two historical winter wheat
92 datasets, namely the panels of Triticeae Genome (TG) (Bentley et al. 2014) and Wheat
93 Association Genetics for Trait Advancement and Improvement of Lineages (WAGTAIL)
94 (Fradgley et al. 2019). The WAGTAIL panel is used only as a replicate RALLY analysis. Within
95 the TG panel, we identify 22 RALLY QSLs and compare them to the GWAS QTLs from Ladejobi
96 et al. (2019). Some notable QSLs include one in 2B which coincides with *Ppd-B1* (Mohler et al.
97 2004), *Yr7/Yr5/YrSP* (Marchal et al. 2018) and alien introgression from *Triticum timopheevii*
98 (Tsilo et al. 2008, Martynov et al. 2018), as well as another in 6A that coincides with *TaGW2* (Su
99 et al. 2011), *Rht24* (Würschum et al. 2017) and *Rht25* (Mo et al. 2018). To further support the
100 RALLY QSLs, we show that all 22 QSLs have non-zero local heritabilities for at least one trait.
101 Next, we find clear directional selection in traits like flowering time, lodging, yield, plant height
102 and grain protein content by comparing the signs of predicted marker allele effects with their
103 directions of allele frequency change as given by RALLY. By extending the results to pairs of
104 traits, we identify the selection priorities. For example, more ears with lighter grains have been
105 preferred over fewer ears with heavier grains. Finally, we employ the multivariate breeder's
106 equation (Lande and Arnold 1983) to estimate selection parameters, although our results
107 suggest a limited use in modern crops, in contrast to its original application in evolutionary
108 studies. Overall, we have shown that many major genomic regions have been extensively used

109 in winter wheat breeding and we suggest that future selection should emphasize on improving
110 other unexplored genomic regions.

111

112 **Materials and Methods**

113 **Population simulation with and without selection**

114 We initiated our population simulation in a fictitious species with 10 chromosomes
115 ([Figure 1](#)). The genetic lengths of the chromosomes were set from 100 to 280 centiMorgans
116 (cM) with an increment of 20 cM in subsequent chromosomes. The populations spanned over
117 50 generations (years) with and without selection. All the simulations were performed using the
118 “AlphaSimR” package (Gaynor et al. 2021) in R (R Core Team 2021). We first created 32 inbred
119 founders using the *runMac*s function and we placed one marker (segregating site) at every 0.1
120 cM. Two causal quantitative trait loci (QTLs) were chosen randomly from the markers at each
121 frequency ranging from 1/32 to 16/32, which resulted in 32 QTLs. The QTL effects were drawn
122 from an approximately negative binomial distribution such that the rarer QTL alleles have larger
123 effects than the more common QTL alleles ([Figure 1](#)). We standardized the QTL effects such
124 that the total variance of additive genetic or QTL effects is 1. Phenotypic values for each line
125 were set as a sum of QTL effects and residual effects drawn from a normal distribution of mean
126 0 and variance 1, which is equivalent to a heritability of 0.5.

127 We created selected (S) and unselected (U) populations from the 32 founders using a
128 simplified model that mimics new variety breeding of major crops in Europe. All varieties were
129 derived as F₆ recombinant inbred lines (RILs) from bi-parental crosses. This is equivalent to 4
130 generations of single seed descent (SSD) from an F₂ population. The first 10 generations were
131 created by crossing the initial 32 founders at random. In the subsequent generations, we
132 randomly sampled 32 parents from 6 to 10 generations ago and created 16 bi-parental

133 populations with each having 100 F₆ RILs. By keeping 2 RILs per bi-parental population, we
134 maintained 32 lines at each generation. The 2 RILs were chosen either from the two highest
135 phenotypic values (selected) or randomly (unselected). This step was repeated until the
136 population underwent 55 generations of phenotypic selection. The first 15 generations were
137 discarded as burn-in because none of the parents of the individuals from these 15 generations
138 have been selected, and hence there is no selection-induced allele frequency change. In our
139 simplistic modelling of the plant variety rights (PVRs) system where only a fraction of new lines
140 passing the PVR test, we randomly sampled and retained 8 lines per generation for a total of
141 400 lines that spanned over 50 generations. The simulated populations with and without
142 selection were used in subsequent analyses.

143

144 **RALLY and GWAS in simulated populations**

145 We compared the performances of Regression of Alleles on Years (RALLY) and
146 Genome Wide Association Study (GWAS) when applied to the selected and unselected
147 populations. The model for RALLY was fitted in a logistic regression using the *glm* function in R
148 (R Core Team 2021). The model for GWAS was fitted in a mixed linear model using the
149 *GWASpoly* function in the “GWASpoly” R package (Rosyara et al. 2016).

150 Briefly, the logistic regression model for RALLY can be shown as below:

$$151 \quad z_i = \frac{1}{1 + e^{-(\mu_{RALLY} + \beta_{RALLY,year} X_{year} + \varepsilon_{RALLY})}} \quad \text{[Equation 1]}$$

152 Or, alternatively, the logistic regression model can be rewritten in a linear form as:

$$153 \quad \ln\left(\frac{z_i}{1-z_i}\right) = \mu_{RALLY} + \beta_{RALLY,year} X_{year} + \varepsilon_{RALLY} \quad \text{[Equation 2]}$$

154 Where the model terms are described as below:

155 z_i is a binary variable indicating the absence (0) or presence (1) of an allele at marker i in n
156 lines.

157 μ_{RALLY} is the mean allele frequency in the first year, or y -intercept.

158 $\beta_{RALLY,year}$ is the fixed year effect, or regression coefficient of the year variable.

159 X_{year} is the year variable.

160 ε_{RALLY} is the residual effect with a distribution of $N(0, \sigma_{\varepsilon, RALLY}^2 \mathbf{I})$ and \mathbf{I} is the identity matrix.

161

162 The GWAS model is written as below:

$$163 \quad y = \mu_{GWAS} + \beta_{GWAS,year} X_{year} + g + \beta_i X_i + \varepsilon_{GWAS} \quad \text{[Equation 3]}$$

164 Where the model terms are described as below:

165 y is the trait values in n lines.

166 μ_{GWAS} is the mean of trait value.

167 $\beta_{GWAS,year}$ is the fixed year effect.

168 X_{year} is the year variable.

169 g is the random genetic background effect with a distribution of $N(0, \sigma_g^2 \mathbf{K})$ and \mathbf{K} is the additive
170 genetic relationship matrix.

171 β_i is the fixed allele effect at marker i .

172 X_i is the number of alleles at marker i .

173 ε_{GWAS} is the residual effect with a distribution of $N(0, \sigma_{\varepsilon, GWAS}^2 \mathbf{I})$ and \mathbf{I} is the identity matrix.

174

175 In the given models, the terms of interest are $\beta_{RALLY,year}$ and β_i in RALLY and GWAS,
176 respectively. The term significances are determined by their corresponding standard normal Z -
177 statistics at a Bonferroni corrected threshold of $P = 0.05$. Due to how the populations are
178 simulated, some markers may not segregate in all the populations. These markers, along with
179 the QTLs and other markers that are highly linked ($r^2 > 0.99$) to QTLs, were removed from the
180 RALLY and GWAS analyses. The simulations were repeated for 100 iterations and the models
181 were fitted for each simulated population separately.

182

183 **Model correction by parametric control (PC)**

184 In the previously described naïve RALLY model (Equation 1 and 2), the RALLY test
185 statistics may be inflated by population structure arising from consanguinity and population
186 stratification. These factors can prevent a proper separation of markers under selection or drift if
187 they are not addressed. To control for the inflation, we used a combined approach of genomic
188 control (GC) (Devlin and Roeder 1999) and delta control (DC) (Gorroochurn et al. 2006) which
189 we call parametric control (PC). In the absence of confounding factors, we expect the null test
190 statistics (Z -scores) to be distributed as $N(0,1)$. However, in the presence of population
191 structure, the distribution of null test statistics becomes $N(\delta, \sigma)$. As the terms imply, DC controls
192 the inflation in mean δ and GC controls the inflation in standard deviation σ . If we can estimate
193 δ and σ , we can adjust the test statistics as the following:

$$194 \quad Z_{adj} = \frac{Z - \delta}{\sigma} \quad [\text{Equation 4}]$$

195 We used a maximum likelihood (ML) approach to estimate δ and σ . For any value of Z ,
196 both positive and negative signs are equally likely because the regression coefficient of one
197 allele has the same magnitude but opposite sign of the other allele. Therefore, we can construct
198 a composite likelihood function from two standard normal probability density functions that

199 account for positive and negative Z values. The likelihood function is shown in Equation 5
200 below. To simplify the calculation, we used the log likelihood function as described in Equation 6
201 below. We computed δ and σ for an n -vector of Z values by either maximizing the log likelihood
202 function, or equivalently, minimizing the negative log likelihood function using the “nlm” package
203 in R (R Core Team 2021).

$$204 \quad f(Z|\delta, \sigma) = \prod_{i=1}^n \frac{1}{\sigma\sqrt{2\pi}} \cdot \frac{1}{2} \cdot \left(e^{-\frac{(Z_i-\delta)^2}{2\sigma^2}} + e^{-\frac{(-Z_i-\delta)^2}{2\sigma^2}} \right) \quad \text{[Equation 5]}$$

$$205 \quad l(\delta, \sigma) = \ln(f(Z|\delta, \sigma)) = n \cdot \ln\left(\frac{1}{\sigma\sqrt{2\pi}}\right) + \sum_{i=1}^n \ln\left[\frac{1}{2} \left(e^{-\frac{(Z_i-\delta)^2}{2\sigma^2}} + e^{-\frac{(-Z_i-\delta)^2}{2\sigma^2}} \right)\right] \quad \text{[Equation 6]}$$

206 An important factor in PC is the selection of null marker sets for calculating the inflation
207 factors for adjusting the test statistics. The most conservative approach is to use all markers as
208 the null, but this approach is unrealistic as it results in over-correction when the selection is
209 strong and prevalent across the whole genome. Therefore, PC is best estimated from markers
210 that have not undergone selection, although it is paradoxical given that such markers are
211 unknown at this stage. As a compromise, we may assume that the allele frequency differences
212 between first and last years are larger for markers under selection than drift. This assumption is
213 reasonable for a modern breeding population that has undergone intensive selection. We first
214 predicted the allele frequency change for each marker using the RALLY model and then
215 identified the null marker set from markers that fall below various thresholds of allele frequency
216 change. We tested the thresholds ranging from 0.05 to 0.50 at an increment of 0.01, in which
217 the thresholds of 0.05 and 0.50 correspond to 40% and 99% of the total markers respectively.
218 Unfortunately, because the variance of allele frequency change, $\sigma_{\Delta p}^2 = p(1-p)/2N$, is largest
219 when the initial allele frequencies are intermediate (Falconer and Mackay 1996), a loss in
220 RALLY's power to distinguish between weak selection signal and drift at those markers is
221 unavoidable.

222

223 **Detection limits of RALLY**

224 We estimated the detection limits of RALLY using a simple example that is based on the
225 simulated populations as described previously. We considered a QTL marker and five other
226 proximal markers that are 1, 2, 3, 4 and 5 cM away. The initial QTL frequencies were set to 1/32
227 to 16/32 with an increment of 1/32, and all possible marker-QTL haplotype frequencies were
228 considered. We modelled selection on the QTL by increasing QTL initial frequency to the final
229 frequency of 31/32 over 50 generations according to either a logistic or linear distribution.
230 Consequently, the proximal markers experienced hitch-hiking effect due to the selection on
231 QTL. Assuming an infinite population size, recombination is the sole factor that is responsible
232 for the hitch-hiking effect, which allowed us to model the change in allele frequencies of the
233 proximal markers. Non-recombinants are inherited at a probability of $1 - r$ and recombinants
234 are inherited at a probability of r . From this, we derived the expected allele frequencies for the
235 proximal markers at each generation. Next, we randomly sampled 8 individuals per generation
236 using a binomial distribution with the expected frequencies as the sampling probabilities. This
237 step was repeated for 100 times for each tested marker-QTL haplotype frequencies. A more
238 detailed description of this is provided in Figure S1.

239

240 **RALLY in two wheat panels**

241 We first applied the RALLY approach in the Triticeae Genome (TG) panel (Bentley et al.
242 2014, Ladejobi et al. 2019) as a proof of concept. The TG panel has 344 winter wheat varieties
243 from the UK, France and Germany that were released between 1948 and 2007 (Figure S2),
244 which is ideal for analyzing selection over time in modern wheat breeding. We retained 333
245 varieties that were in common between the TG panel data derived from DArT markers (Bentley

246 et al. 2014) and genotype-by-sequencing (GBS) markers (Ladejobi et al. 2019). The DArT
247 marker data was only used in a later analysis for estimating multivariate selection parameters.
248 From the initial 41,861 GBS markers, we removed 3,009 markers that are in high linkage
249 disequilibrium (LD) ($r^2 > 0.2$) with markers from other chromosomes which left us with 38,852
250 markers. These markers were positioned according to the IWGSC RefSeq v1.0 genome
251 assembly. Here, we applied a similar model to Equation 2 with an additional fixed effect to
252 account for the country of origin. We identified the year regression coefficients, applied the
253 same level of PC as identified from the simulation to adjust the test statistics, and determined
254 the significance at a Bonferroni-corrected threshold of 0.05.

255 Next, we replicated the analysis in the WAGTAIL panel (Fradgley et al. 2019) to test
256 RALLY performance in a different sampling panel of modern wheat varieties. The WAGTAIL
257 panel has 403 winter wheat varieties of mostly UK origin that were released between 1916 and
258 2010. Of the 403 varieties, 283 originated from the UK, 51 from France, 34 from Germany and
259 35 from other countries including Australia, Belgium, Canada, Denmark, the Netherlands,
260 Sweden, Switzerland, and United States. There were 99 overlapping varieties between the TG
261 and WAGTAIL panels. Since the WAGTAIL panel was genotyped using the wheat 90k array
262 (Wang et al. 2014) and did not immediately have physical map positions for direct comparison
263 with the TG panel, we identified the physical map positions from the IWGSC RefSeq v1.0
264 annotation file. We retained 5,592 out of 26,015 markers that had matching chromosomes
265 between the original WAGTAIL genetic map and the physical map. We also removed 319
266 markers that are in high LD ($r^2 > 0.2$) with markers from other chromosomes which left us with
267 5,273 markers. We applied Equation 2 with an additional fixed country of origin effect to the
268 WAGTAIL panel and computed the year regression coefficients with the same PC and multiple
269 testing correction to the test significances.

270

271 **Estimating local heritabilities from RALLY QSLs**

272 We clustered the significant markers identified from RALLY into groups based on the
273 extent of LD surrounding the markers. Because genomic markers are not completely
274 independent, some significant markers may be tagging the same QSLs. Starting with the most
275 significant (focal) markers within each chromosome, we assigned markers that have $r^2 > 0.2$
276 with the focal marker to the same group. To avoid incorrectly mapped markers, we require the
277 groups to have a minimum of 10 markers in the TG panel and 5 markers in the WAGTAIL panel
278 due to lower marker density. As a trade-off, there may be bias against genomic regions with
279 sparse marker density such as the D-genome. We repeated the process for the next significant
280 marker that has not been assigned to any group until all significant markers have been
281 assigned. Lastly, we merged all overlapping groups.

282 We estimated the local heritabilities (h_l^2) for each QSL in the TG panel using the
283 genomic heritabilities partitioning method that was introduced by Schork (2001) and Visscher et
284 al. (2007). QSLs with non-zero h_l^2 would support the hypothesis of selection over drift for the
285 observed change in allele frequency. The TG panel includes 12 traits: Flowering Time (FT),
286 Lodging (LODG), Yield (YLD), Plant Height (HT), Grain Protein Content (PROT), Winter Kill
287 (WK), Awns (AWNS), Specific Weight (SPWT), Total Grain Weight (TGW), Ears per m² (EM2),
288 Tiller Number (TILL) and Maturity (MAT) (Bentley et al. 2014, Ladejobi et al. 2019). We were not
289 able to estimate the h_l^2 in the WAGTAIL panel since we did not have multi-trait data for the
290 WAGTAIL panel. For each trait and QSL combination, we estimated the h_l^2 from the following
291 mixed model fitted using the *mmer* function from the “sommer” package (Covarrubias-Pazaran
292 et al. 2016) in R (R Core Team 2021):

$$293 \quad y = \mu + X\beta + g_0 + g_i + \varepsilon \quad \text{[Equation 7]}$$

294 Where the model terms are described as below.

295 y is a vector of phenotypic trait values for n varieties.

296 μ is the trait mean.

297 X is an $n \times 2$ matrix of incidence matrix for the fixed year and country of origin effects.

298 β is a vector of length 2 of the fixed year and country of origin effects.

299 g_0 is a vector of length n of the random genetic effect due to relationship among varieties
300 calculated from markers not in group i , and it follows a distribution of $N(0, \sigma_{g,0}^2 K_0)$.

301 g_i is a vector of length n of the random genetic effect due to relationship among varieties
302 calculated from markers in group i , and it follows a distribution of $N(0, \sigma_{g,i}^2 K_i)$.

303 ε is a vector of length n of the random residual effect under a distribution of $N(0, \sigma_\varepsilon^2 I)$.

304 After each model was fitted, we calculated the h_l^2 as $\frac{\sigma_g^2}{\sigma_g^2 + \sigma_\varepsilon^2}$. For any trait, we identified the
305 non-zero h_l^2 groups ($h_l^2 > 0.001$) and refitted a new mixed model with all the non-zero h_l^2
306 groups. The model is shown as below with the similar terms as explained in Equation 7.

307
$$y = \mu + X\beta + g_0 + \sum g_i + \varepsilon \quad \text{[Equation 8]}$$

308 From Equation 5, we estimated the new h_l^2 as $\frac{\sigma_{g,i}^2}{\sum \sigma_{g,i}^2 + \sigma_\varepsilon^2}$ and used these as the final
309 estimated h_l^2 for each trait and group combination.

310

311 **Associating marker effects with alleles that are increasing over time**

312 We estimated the marker allele effects for each trait in the TG panel using ridge
313 regression (RR) (Hoerl and Kennard 1970) and least absolute shrinkage and selection operator
314 (LASSO) (Tibshirani 1996) approaches. For the RR approach, we used the *mixed.solve* function

315 from the “rrBLUP” package (Endelman 2011) in R (R Core Team 2021). For the LASSO
316 approach, we used the *cv.glmnet* function from the “glmnet” package (Friedman et al. 2010) in
317 R (R Core Team 2021). In both approaches, we fitted a multiple linear regression model as
318 shown below:

$$319 \quad y = \mu + Zu + \varepsilon \quad \text{[Equation 9]}$$

320 Where the model terms are described as below.

321 y is a vector of phenotypic trait values for n varieties.

322 μ is the trait mean.

323 Z is a $n \times p$ matrix of numerical marker genotypes coded as -1, 0 and 1 for homozygous first
324 allele, heterozygous and homozygous second allele, respectively. The number of markers is p .

325 u is a vector of marker allele effects. In RR, u is estimated from minimizing the loss function of

326 $L_{RR}(u) = \|y - \mu - Zu\|^2 + \lambda\|u\|^2$ where $\lambda = \sigma_\varepsilon^2 / \sigma_u^2$ and $u \sim N(0, \sigma_u^2 I)$ (Endelman 2011). In

327 LASSO, u is estimated from minimizing the loss function of $L_{LASSO}(u) = \|y - \mu - Zu\|^2 + \lambda\|u\|$

328 where λ is determined from the default 10-fold cross validations in *cv.glmnet* (Friedman et al.

329 2010). In addition, the multivariate LASSO model in “glmnet” was used to ensure that the effects

330 for all traits are estimated from the same set of chosen markers.

331 ε is a vector of residual effects that follows a distribution of $N(0, \sigma_\varepsilon^2 I)$.

332 For each trait j and marker k , we identified $\tilde{d}_{j,k}$ which is the effect direction for the allele

333 that is increasing in frequency over time, as follows: first, we determined $\tilde{u}_{j,k}$ which is the

334 direction of marker allele effect estimated from either RR or LASSO using the *sign* function in R

335 (R Core Team 2021). This resulted in $\tilde{u}_{j,k} = -1$ for negative effect, $\tilde{u}_{j,k} = 0$ for no effect and

336 $\tilde{u}_{j,k} = 1$ for positive effect. Next, we determined $\tilde{\beta}_{j,k}$ which is the direction of year regression

337 coefficient estimated from RALLY. This resulted in $\tilde{\beta}_{j,k} = -1$ for decreasing allele and $\tilde{\beta}_{j,k} = 1$
338 for increasing allele. Because the marker alleles were coded similarly in the RALLY and marker
339 BLUP models, we could calculate $\tilde{d}_{j,k}$ as $\tilde{u}_{j,k} \times \tilde{\beta}_{j,k}$ directly. $\tilde{d}_{j,k} = 1$ suggests that the increasing
340 allele has a positive effect and $\tilde{d}_{j,k} = -1$ suggests that the increasing allele has a negative
341 effect. $\tilde{d}_{j,k} = 0$ is only possible in LASSO due to variable selection, which simply implies that
342 there is no effect. For any trait, an excess of either $\tilde{d}_{j,k} = -1$ or $\tilde{d}_{j,k} = 1$ across all markers
343 indicates a possible directional selection.

344 For a pair of traits j_1 and j_2 , we calculated $\tilde{d}_{j_1,j_2,k} = [\tilde{d}_{j_1,k} \quad \tilde{d}_{j_2,k}]$ which is the pairwise
345 effect direction for the increasing allele. $\tilde{d}_{j_1,j_2,k} = [1 \quad 1]$ implies that the increasing allele has
346 positive effects on both traits, $\tilde{d}_{j_1,j_2,k} = [1 \quad -1]$ or $\tilde{d}_{j_1,j_2,k} = [-1 \quad 1]$ implies that the increasing
347 allele has a positive and a negative effect on either trait, and $\tilde{d}_{j_1,j_2,k} = [-1 \quad -1]$ implies that the
348 increasing allele has negative effects on both traits. By forming a contingency table from the
349 counts of all four possible $\tilde{d}_{j_1,j_2,k}$ combinations, we tested for selection-related interaction
350 between the pairs of traits using a $\chi^2_{df=1}$ test in the results involving LASSO. We did not test the
351 results involving RR because the marker effects are not independent.

352

353 **Estimating multivariate selection parameters**

354 We estimated the multivariate selection parameters in the TG panel using the
355 multivariate breeder's equation of $\Delta Z = G\beta_{sel}$ (Lande and Arnold 1983). We obtained the
356 selection response (ΔZ), genetic variance-covariance matrix (G) and phenotypic variance-
357 covariance matrix (P) from the trait and marker data. Next, we solved the multivariate breeder's
358 equation for the selection gradient β_{sel} and the equations of $S = P\beta_{sel}$ and $i = S/\sqrt{diag(P)}$ for
359 the selection differential (S) and selection intensity (i) (Falconer and Mackay 1996). Lastly, we

360 decomposed the multivariate selection parameters into direct and indirect partitions as a method
361 to quantify the direct and indirect historical selection in the TG panel. As a check, we repeated
362 the same process in a simulated example. Complete details on the methods on estimating
363 multivariate selection parameters are provided in the Supplementary Methods.

364

365 **Results**

366 **RALLY and GWAS in simulated populations**

367 We tested RALLY's ability in identifying selection- or drift-induced marker allele
368 frequency changes in simulated populations with (S) and without (U) selection ([Figure 1](#)) by
369 varying the degree of parametric control (PC). Briefly, PC combines genomic control (GC)
370 (Devlin and Roeder 1999) and delta control (DC) (Gorroochurn et al. 2006) to correct for
371 inflation in test statistics due to population structure. Details on the PC approach and
372 simulations are described in the Materials and Methods section. Across all tested allele
373 frequency change thresholds (t) for null marker set, setting $t > 0.11$ produced better control of
374 test statistics (significant markers in S < 1.867%, U < 0.109%) than without any correction
375 (significant markers in S = 1.942%, U = 0.089%) ([Figure 2A](#), Table S1). At $t = 0.15$, we found
376 little significance in the unselected population across all 100 simulations with some inevitable
377 loss of significance in the selected population (significant markers in S = 0.994%, U = 0.012%)
378 (Table S1). This result suggests that PC at this threshold can reasonably separate out the true
379 selection signals from drift in our simulation. To err on the cautious side, we used a higher
380 threshold of $t = 0.20$ in the simulation, TG and WAGTAIL panels.

381 We evaluated the QSL/QTL mapping performances of RALLY and GWAS in the
382 simulated populations with selection ([Figure 1](#)) and found a higher mapping power in RALLY
383 over GWAS ([Figure 2](#)). Across the 100 simulations, we found that the individual significant

384 markers are rarely shared between RALLY and GWAS ([Figure 2B](#)), and even less likely to be
385 found in GWAS but not RALLY ([Figure 2D](#)). Most of the significant markers are found in RALLY
386 but not GWAS ([Figure 2C](#)). The low number of significances in GWAS is likely because the
387 simulated QTLs have small effects and low heritabilities, which is common for quantitative traits.
388 The heritabilities for the largest QTLs are approximately 0.030 and the smallest QTLs are
389 approximately 0.002. An additional intention of having low heritabilities is to reduce the fixation
390 rate of QTL due to selection and prevent pre-matured fixation of QTL in the simulated
391 population.

392 We repeated the RALLY and GWAS analyses in the unselected populations as a control
393 for the same analyses in the selected populations ([Figure 2](#)). On average across all 100
394 simulations, RALLY identifies 0.1 significant markers out of 19,000 total markers in the
395 unselected population compared to 104.5 significant markers in the selected population. This
396 result suggests that less than 0.1% of the significant markers in the selected population are
397 likely caused by drift instead of selection. In the selected population, there are more significant
398 markers (means of 99.4 versus 5.1) that are close to the QTLs (≤ 5 cM) than far (> 5 cM)
399 ([Figure 2B-C](#)). Assuming that all 32 QTLs are selected and all markers within 5 cM of the QTLs
400 experience hitch-hiking effect, there should be a maximum of 3,200 significant markers in the
401 selected population. However, the number of significant markers is much lower in reality
402 because: (1) the selection force is proportional to the QTL effects ([Figure S3](#)), (2) the hitch-
403 hiking effect depends on the initial marker-QTL haplotype distribution ([Figure S1](#)), and (3) the
404 hitch-hiking effect decreases as genetic distance increases. On the other hand, GWAS
405 performance remains similar between the selected and unselected populations ([Figure 2](#)).

406

407 **Detection limits of RALLY**

408 Following from the previous simulation, we investigated the relationship between QTL
409 under selection and its proximal markers and the results suggested a detection limit of
410 approximately 5 cM (Figure S4). Here, we considered 10 markers that are evenly spaced
411 between 1 to 10 cM away from a QTL and evaluated how these marker allele frequencies
412 change as a result of increasing QTL frequency. Because the markers are linked to the QTL, we
413 expect their frequencies to follow the QTL frequency in an inversely proportional way according
414 to their genetic distances from the QTL. This process is commonly known as hitch-hiking, and it
415 is an important consideration for RALLY because hitch-hiking markers are more likely to be
416 genotyped than the true QTLs. Curiously, our results suggest that the ability of RALLY in
417 identifying significant hitch-hiking markers depends on the QTL-marker haplotypes, QTL initial
418 frequency, and genetic distance between QTL and marker (Figure S4). With all factors
419 considered, RALLY rarely detects significance beyond 5 cM although our previous results
420 showed that some long-range significances may still be present ([Figure 2B](#)). A possible
421 explanation for this is when multiple QTLs co-localize into one major QTL haplotype, which may
422 amplify the significances of surrounding markers.

423

424 **RALLY in two wheat panels**

425 We mapped 22 significant QSLs (Bonferroni corrected $p < 0.05$) across 14
426 chromosomes in the Triticeae Genome (TG) panel using RALLY ([Table 1](#), [Figure 3](#), Figure S5,
427 File S1). Because the distances between significant markers and true QTLs are unknown, we
428 used a linkage disequilibrium (LD) measure of $r^2 > 0.2$ as a method to identify the genomic
429 boundaries that the significant markers tag. This method resulted in QSL intervals ranging from
430 1.46 Mb to 774.73 Mb with a mean of 148.74 Mb. Given the large blocks of genomic regions

431 and a previously approximated RALLY detection limit of 5 cM, many of the QSLs are likely to fall
432 within low recombination regions. QSLs in high recombination regions are harder to map due to
433 the lack of markers tagging the causative QTLs. Besides, sustained selection is more likely to
434 be observed on multiple weakly favorable alleles in low than high recombination regions.

435 Of the 22 QSLs, 12 co-localize with previously mapped QTLs using GWAS (Ladejobi et
436 al. 2019) in the TG panel ([Table 1](#), [Figure 3](#), [Figure 4](#), Table S2). QSLs/QTLs found in both
437 RALLY and GWAS indicate that their effects are likely beneficial and have been selected during
438 the breeding process. QSLs unique to RALLY suggest that their effects might be too small for
439 GWAS to detect or the specific traits have not been analyzed for GWAS. QTLs unique to GWAS
440 suggest that they are still segregating in the population, which could be due to various reasons
441 like recent introduction into the breeding population and linkage drag.

442 A literature search showed that RALLY QSLs occur in both well-characterized and novel
443 genomic regions in winter wheat (Table S3). The most significant RALLY QSL-6 mapped to a
444 large region in chromosome 2B: 11 – 230 Mb, which includes *Ppd-B1* (Mohler et al. 2004) and
445 multiple resistance loci of *Yr5*, *Yr7* and *YrSP* (Marchal et al. 2018). Another major QSL-16
446 mapped to a large region in chromosome 6A: 62 – 545 Mb, which contains *TaGW2* (Su et al.
447 2011) and the GA-responsive dwarfing genes of *Rht24* (Würschum et al. 2017) and *Rht25* (Mo
448 et al. 2018). Interestingly, the durum wheat dwarfing gene *Rht14/16/18* resides in the same
449 genomic region, although it remains to be tested whether it is allelic to *Rht24* (Haque et al.
450 2011). A recent EnvGWAS in winter wheat by Sharma et al. (2021) also mapped to the same
451 genomic region (6A: 396 Mb) but without mention of any *Rht* candidate gene. On a broader
452 scale, 16 RALLY QSLs co-localize with the recently identified meta-QTLs on yield and yield-
453 related traits in wheat (Yang et al. 2021). 9 RALLY QSLs overlap with the QTLs identified from a
454 Multi-parental Advanced Generation Inter-Cross (MAGIC) population of 16 diverse UK winter
455 wheat varieties (Scott et al. 2021).

456 In addition, we found 11 RALLY QSLs that overlap with known alien and non-alien
457 introgressions in wheat (Cheng et al. 2019). These include major introgressions like the 2A: 0 –
458 11 Mb from *Aegilops ventricosa* (Robert et al. 1999, Rhoné et al. 2007) and 2B: 90 – 749 Mb
459 from *Triticum timopheevii* (Tsilo et al. 2008, Martynov et al. 2018). These two introgressions
460 were shown to segregate among the UK winter wheat varieties by Scott et al. (2021). Because
461 alien introgressions tend suppress recombination (Gill et al. 2011), they can be easily mapped
462 using RALLY. Considering all overlaps in results between RALLY and the studies described
463 thus far, we found 19 RALLY QSLs that can be traced to at least one study.

464 In the WAGTAIL panel, we mapped 19 significant QSLs across 13 chromosomes using
465 RALLY (Table S4, Figure S6, File S1). We used the same approach as we did with the TG
466 panel to identify the boundaries of these significant QSLs. With 99 varieties in common between
467 the TG and WAGTAIL panels, we expect a high number of overlapping QSLs. 10 out of 19
468 QSLs in the WAGTAIL panel matched with 10 out of 22 QSLs in the TG panel ([Figure 4](#)), which
469 is approximately one-half overlap between them. Given that the TG panel was genotyped using
470 GBS (Elshire et al. 2011) while the WAGTAIL panel was genotyped using the 90k array (Wang
471 et al. 2014), the genotyping and mapping quality of these two panels are likely different. This
472 may partially explain why the results from the TG and WAGTAIL panels did not fully overlap.
473 Another possible reason is that the distributions of countries of origins differ in the two panels in
474 which the TG panel is more homogeneous than the WAGTAIL panel.

475

476 **Local heritabilities in the RALLY QSLs**

477 We calculated local heritabilities for the 22 RALLY QSLs as a support for possible
478 selection over drift at these QSLs ([Table 2](#), [Figure 5](#)). We found that all 22 QSLs have non-zero
479 local heritabilities for at least one trait. We tested for non-zero in the local heritabilities using a

480 likelihood ratio test to compare between the mixed models with and without QSLs (Santantonio
481 et al. 2019). However, most of the tests were non-significant due to low power (Table S5). The
482 tests for QSLs collectively showed significance in 5 out of 12 traits, which comes at a cost of
483 losing the test on individual QSL in exchange for a slightly higher power. In an extreme example
484 with a total heritability of 0.379, QSL-16 at 6A: 89,355,276 is associated with 8 traits and found
485 to co-localized with all other previously mentioned results. While it is possible that the underlying
486 candidate genes *TaGW2* (Su et al. 2011), *Rht24* (Würschum et al. 2017) and *Rht25* (Mo et al.
487 2018) have pleiotropic effects that are beneficial for wheat breeding, we cannot exclude the
488 possibility of additional genes that provide breeding advantages in the same haplotype block.
489 Nonetheless, given that QSL-16 has already played a major role in wheat breeding, it is unlikely
490 to be useful for future breeding. The genomic region with the next largest total heritability of
491 0.226 is located in QSL-2 at 1A: 138,028,803. While no known gene has been mapped around
492 QSL-2, results from our analysis and others (Cadalen et al. 1998, Griffiths et al. 2012, Tiwari et
493 al. 2016) suggest that it may contain loci responsible for plant height and grain protein content.

494 Between the cumulative heritabilities explained by these 22 QSLs and the remaining
495 genomic regions, HT and TGW are higher in the QSLs, AWNS is lower in the QSLs and the
496 other 9 traits are about equal ([Table 2](#), [Figure 5](#)). This result highlights the narrow genetic
497 diversity that is often seen in modern varieties (Reif et al. 2005) due to the repeated use of
498 identical favorable haplotypes in wheat breeding. Fortunately, the remaining “unselected”
499 genomic regions for important traits like yield, grain protein content and plant height are not fully
500 devoid of heritabilities. There is still room for varietal improvement without the introduction of
501 favorable exotic alleles in the short term, which suggests that it might be better to devote some
502 of the resources in pre-breeding on these genomic regions instead. For traits like TGW and
503 TILL, breeders may need to look for alternative genetic resources to compensate for the lack of
504 diversity.

505

506 **Marker effects of alleles that are increasing over time**

507 We evaluated the marker allele effects using the prediction models from Ridge
508 Regression (RR) and Least Absolute Shrinkage and Selection Operator (LASSO). Across all 12
509 traits, RR resulted in higher prediction accuracy than LASSO although the differences were
510 comparable in some traits (Figure S7 and S8). Despite that, we retained the results from both
511 approaches because the variable selection step in LASSO is important for a follow-up test
512 involving trait pairs.

513 We examined the marker allele effect directions for increasing alleles and found
514 excesses in one over another direction across each of the 12 traits ([Figure 6](#), Figure S9). We
515 first partitioned the markers based on their RALLY significance into three groups: (1) markers
516 with p-values lower than the Bonferroni corrected threshold of 0.05, (2) markers with p-values
517 between 0.05 and the Bonferroni corrected threshold of 0.05, and (3) markers with p-values
518 higher than 0.05. The results from using either RR ([Figure 6](#)) or LASSO (Figure S9) are similar
519 although the differences across the significance groups in LASSO are less pronounced, i.e.
520 there are more differences between group 1 and 2 in RR than LASSO results. This might be
521 due to LASSO selected markers having weak but small, non-significant changes in allele
522 frequencies over time. Within the RR results, the excesses in effect directions are strongest in
523 the significance group 1 and weakest in the significant group 3, which suggest that the excesses
524 can be related to the favored direction of selection. The lack of excesses in significance group 3
525 implies that favorable and unfavorable alleles are still segregating about equally in the
526 unselected genomic regions.

527 Across all 12 traits, the excesses agree with our expectation of traits that are important
528 in wheat breeding. The most extreme example is yield (YLD) where both the RR and LASSO

529 results show a near complete excess of positive effects in the increasing alleles in significance
530 group 1. As shown previously by Mackay et al. (2011), the genetic gain in the UK winter wheat
531 yield has been rising steadily over time. The next four traits with strong excesses are flowering
532 time (FT), lodging score (LODG), plant height (HT) and grain protein content (PROT). FT,
533 LODG and HT are favored for lower trait values, and thus the increasing alleles have excesses
534 in negative effects. On the contrary, higher PROT is valuable for bread making quality, which is
535 unfortunately going in the opposite direction due to a strong negative genetic correlation with
536 yield (Scott et al. 2021). This result suggests that the selection for higher yield is a lot stronger
537 than the selection for higher grain protein content. In the remaining traits, the excesses are
538 smaller and less obvious given the variations seen from RR and LASSO results, which suggests
539 that directional selection is likely weak for these traits.

540 By comparing the effect directions for increasing alleles in pairs of traits, we identified
541 the priorities of traits under selection ([Table 3](#), Table S6 and S7, [Figure 7](#)). Taking YLD and
542 PROT for example, there is a strong excess for alleles with positive YLD but negative PROT.
543 This result reiterates the priority of YLD over PROT in wheat breeding. Between TGW and EM2,
544 there is an excess for alleles with positive EM2 and negative TGW which suggests that more
545 ears with lighter grains are preferred over fewer ears with heavier grains. In a different
546 perspective, the results here also highlight the constraints imposed by genetic correlations
547 across traits. For example, there is a small proportion of alleles with the same effect directions
548 for YLD and PROT. These alleles could be used in breeding high YLD and PROT varieties,
549 although it is still important to consider the possibility that these alleles could be unfavorably
550 associated with other traits.

551

552 **Multivariate selection parameters**

553 In contrast to a genomic-centric approach that has been described thus far, the
554 multivariate selection parameters may provide an alternative, trait-focused perspective on the
555 historical selection of winter wheat represented by the TG panel. We found a strong
556 misalignment between the selection response (ΔZ) and gradient (β_{sel}) where the directions of the
557 vectors' elements are the opposite in 5 out of 12 traits (Table S8). If the selection parameters
558 are estimated accurately, such divergence may imply an inefficient selection process. In
559 addition, we partitioned the selection response (ΔZ), differential (S) and intensity (i) into direct
560 and indirect components to quantify the amount of each selection parameter that is directly due
561 to the available variation within a trait or indirectly due to the covariation with other traits. In an
562 example with HT, we found positive direct effects in ΔZ , S and i , which contradicts the known
563 selection on dwarfing genes like *Rht1*, *Rht2* and *Rht24* (Pearce et al. 2011, Würschum et al.
564 2017). Given the uncertainties in the multivariate selection parameters, we have provided the
565 full results in the Supplementary Results and we advise to treat these estimates with caution.

566 Following the results, we investigated the possible causes of issues in estimating
567 multivariate selection parameters using a simulated example with a single generation of
568 selection involving three genetically correlated traits. First, we found that the genetic variances
569 and covariances (G) estimated from mixed linear model were close to the true simulated values
570 but with low precision (Table S9, Figure S10). Next, we computed the selection parameters (ΔZ ,
571 β_{sel} , S , i) from the simulation directly, true G and estimated G , which are referred to as true,
572 realized and estimated values, respectively. Given the imprecise estimates of G , we observed
573 lower correlations between the estimated and true values than between the realized and true
574 values (Table S9, Figure S11-S16). Despite using the true G , the realized values still failed to
575 match the true values perfectly, which indicates that the deviations in realized ΔZ are carried
576 over into the other selection parameters that are estimated downstream.

577

578 **Discussion**

579 **Advantages and disadvantages of RALLY**

580 RALLY has a major feature of being a trait-free method for mapping QSLs; however, this
581 feature is a double-edged sword. For any population, RALLY involves only a single, relatively
582 simple logistic regression analysis. In contrast, GWAS requires either multiple, simple mixed
583 model analyses for each trait or a single, yet computationally intensive multi-trait analysis.
584 Unlike any other trait-based mapping methods, the QSLs identified through RALLY are not
585 restricted to only traits that are scored. While this makes RALLY a convenient method, the
586 results do not inform us which traits the QSLs are associated with. In this regard, we will need to
587 rely on other trait-based analyses like GWAS or genomic variance partitioning (Schork 2001,
588 Visscher et al. 2007) to relate QSLs to traits. This additional step is not restricted to the same
589 population as the QSL-trait information can be drawn from other studies such as GWAS on 47
590 traits in the wheat MAGIC diverse population (Scott et al. 2021). Therefore, RALLY can function
591 as a replication of results from other studies.

592 As a kinship-free method, RALLY avoids any potential issues that may arise from the
593 use of genomic relationship matrix (GRM) in mixed linear models. Recently, kinship estimates
594 have been shown to be biased under complex population structure (Ochoa and Storey 2021),
595 which can arise due to selection and migration of materials across breeders and countries.
596 Besides, kinship estimates depend on the assumption that the alleles frequencies observed in
597 the study population are representative of the reference or base population. For a population
598 that has only experienced weak to no selection, the mean of genome-wide marker variance
599 might be a reasonable approximation to the reference population. But, in populations under
600 strong selection like modern crop varieties, the deviation between observed and true (reference)
601 distribution of allele frequencies may not be trivial. Jiang et al. (2021) showed that the kinship

602 estimates are biased when the observed distribution of allele frequencies fails to match the true
603 distribution. In addition, a similar study on populations of modern wheat and barley varieties
604 suggested that their kinship estimates may be biased due to long period of intensive selection
605 (Sharma et al. 2021). However, the bias impacts on mapping power in GWAS and accuracy of
606 variance component estimates remain to be evaluated.

607 Given that RALLY is designed specifically for mapping QSLs that have been selected
608 over a time period, there may be limited utilities outside of its target scope. Our RALLY analyses
609 model the change in allele frequency under a logistic distribution, which requires both genomic
610 marker and year of variety release information. So, RALLY cannot be immediately applied to
611 typical artificial mapping populations like bi-parental, nested association mapping (NAM) or
612 MAGIC populations. However, we can extend the use of RALLY by conceptualizing it in its
613 simplest form, which is a regression of marker allele on a variable of interest. For example, we
614 can regress the marker allele on a continuous geographical origin variable such as latitudes and
615 altitudes. The outcomes would directly define alleles that are relevant to local adaptation.
616 Furthermore, the hybrid approach of parametric control (PC) is independent of RALLY and can
617 be used in any genome-wide mapping analyses as a replacement for GRM and mixed linear
618 model.

619

620 **Selection history and future direction in winter wheat breeding**

621 Given the largely incomplete overlap between RALLY and GWAS QSLs/QTLs in the TG
622 panel, GWAS-specific QTLs may not have been directly useful in breeding. Several possible
623 reasons include linkage drag between the QTLs, recent introduction of QTL alleles into the
624 breeding pool, and ineffective selection at those QTLs. In the absence of genome editing to
625 remove unfavorable alleles (Johnsson et al. 2019), linkage drag is unavoidable due the low

626 probability of creating favorable recombinant haplotypes. New QTL alleles are hard to map
627 under RALLY due to low power issue, but it can be improved by including more recent varieties.
628 Ineffective selection is a direct consequence of the selection tendency towards low-hanging
629 fruits. In an extreme example involving a cross between an elite variety and an exotic wild
630 relative, selection is bound to reconstitute the elite genome because of the higher probabilities
631 of favorable alleles in the elite over exotic genomes (Gorjanc et al. 2016). This phenomenon is
632 observed in a large-scale crossing program involving groups of one exotic and two elite parents,
633 in which the resulting lines lost approximately two-thirds of the expected exotic genome (Singh
634 et al. 2021). In this regard, the approach of Origin Specific Genomic Selection (OSGS) (Yang et
635 al. 2020) can be used to specifically target genomic regions outside of RALLY QSLs for
636 selection.

637 The association between directions of allele frequency change and predicted marker
638 effects provides us with an overview of selection priorities ([Figure 6](#) and [7](#)). High yield, short
639 plants, early flowering, reduced lodging and reduced grain protein content are clearly preferred
640 under directional selection. However, there is no obvious directional selection on spikes and
641 grain related traits, which suggests that there is no specific morphology that provides advantage
642 in the breeding practice. The pairwise analysis further demonstrates the selection priorities and
643 genetic correlations between traits. The results can be used to formulate a future breeding
644 direction, for example, breeding for varieties with high yield and grain protein content by
645 focusing on increasing the frequencies of the favorable alleles on both traits. In line with the
646 global interest in shifting towards more sustainable agricultural practice (Hoad 2010), this
647 approach can be extended to include traits relevant to sustainability and climate resilience to
648 better guide the breeding direction.

649

650 **Limited practical use of multivariate breeder's equation**

651 As shown in the results involving the TG panel, the multivariate breeder's equation has
652 limited practical use in estimating selection parameters (Table S8). An important component of
653 the equation is the genetic variance-covariance matrix (G). The assumption that G is constant is
654 likely violated because G should have been calculated from the base population (Walsh and
655 Lynch 2018) rather than a population under selection over a time period. While this violation
656 likely contributes to the poor estimates of the selection parameters, it is not the only source of
657 issue. Variations across two tested genotyping methods (GBS and DArT) resulted in severely
658 different selection parameters (Table S8) even when the G were similar across the two methods
659 (Table S10).

660 Despite fulfilling the assumption of constant G and eliminating the genotyping
661 discrepancy in our simulated example, additional issues remain in estimating selection
662 parameters from the multivariate breeder's equation. We found that the poor estimation of
663 multivariate selection parameters is caused by imprecise G estimated from mixed linear model.
664 However, the estimation of multivariate selection parameters cannot be completely recovered
665 even when the true G is used. This is probably because the multivariate breeder's equation can
666 only capture the means but not the variances of the selection parameters (ΔZ , β_{sel} , S , i). Since
667 the selection parameters are derived sequentially, repeated deviations from the means result in
668 poor estimates of the selection parameters. This issue can be remedied by increasing the
669 sample size, although there is a limit to the sample size due to practicality in breeding practice.
670 Furthermore, the deviation is amplified across multiple generations of selection. Given the multi-
671 layered issues with estimating selection parameters using the multivariate breeder's equation, it
672 is best to limit its use to predict forward for a single generation as a rough guide to selection
673 experiments involving crop varieties.

674

675 **Acknowledgments**

676 We thank Rajiv Sharma, Ian Dawson and David Marshall for helpful discussion on the work.

677

678 **Author Contributions**

679 CJY and IM conceived the work, performed the analyses and wrote the manuscript. OL
680 provided data for the Triticeae Genome (TG) panel. RM and WP provided critical comments. All
681 authors read, revised and approved the manuscript. No external funding was received for the
682 work in this manuscript.

683

684 **Data Availability**

685 The GBS and phenotypic trait data for the TG panel (Ladejobi et al. 2019) were downloaded
686 from doi.org/10.6084/m9.figshare.7350284. The TG panel DArT data (Bentley et al. 2014) and
687 WAGTAIL panel data (Fradgley et al. 2019) were downloaded from [https://www.niab.com/
688 research/agricultural-crop-research/resources](https://www.niab.com/research/agricultural-crop-research/resources). The IWGSC RefSeq v1.0 annotation file
689 containing the physical map positions for the 90k wheat array was downloaded from
690 [https://urgi.versailles.inra.fr/download/iwgsc/IWGSC_RefSeq_Annotations/v1.0/iwgsc_refseqv1.
691 0_Marker_mapping_summary_2017Mar13.zip](https://urgi.versailles.inra.fr/download/iwgsc/IWGSC_RefSeq_Annotations/v1.0/iwgsc_refseqv1.0_Marker_mapping_summary_2017Mar13.zip). Computational analyses were performed using
692 R version 4.1.0. All R scripts used in the analyses can be found at [https://cjiang-
693 sruc.github.io/RALLY](https://cjiang-sruc.github.io/RALLY).

694

695 **Competing Interests**

696 The authors declare no conflict of interest.

697

698 **References**

- 699 1. Bentley AR, Scutari M, Gosman N, Faure S, Bedford F, Howell P, Cockram J, Rose GA,
700 Barber T, Irigoyen J, Horsnell R, Pumfrey C, Winnie E, Schacht J, Beauchêne K, Praud S,
701 Greenland A, Balding D, Mackay IJ (2014) Applying association mapping and genomic
702 selection to the dissection of key traits in elite European wheat. *Theor Appl Genet* 127:
703 2619-2633.
- 704 2. Cadalen T, Sourdille P, Charmet G, Tixier MH, Gay G, Boeuf C, Bernard S, Leroy P,
705 Bernard M (1998) Molecular markers linked to genes affecting plant height in wheat using a
706 doubled-haploid population. *Theor Appl Genet* 96: 933-940.
- 707 3. Cheng H, Liu J, Wen J, Nie X, Xu L, Chen N, Li Z, Wang Q, Zheng Z, Li M, Cui L, Liu Z,
708 Bian J, Wang Z, Xu S, Yang Q, Appels R, Han D, Song W, Sun Q, Jiang Y (2019) Frequent
709 intra- and inter-species introgression shapes the landscape of genetic variation in bread
710 wheat. *Genome Biol* 20: 136.
- 711 4. Covarrubias-Pazaran G (2016) Genome-assisted prediction of quantitative traits using the R
712 package *sommer*. *PLoS One* 11: e0156744.
- 713 5. Decker JE, Vasco DA, McKay SD, McClure MC, Rolf MM, Kim J, Northcutt SL, Bauck S,
714 Woodward BW, Schnabel RD, Taylor JF (2012) A novel analytical method, Birth Date
715 Selection Mapping, detects response of the Angus (*Bos Taurus*) genome to selection on
716 complex traits. *BMC Genomics* 13: 606.
- 717 6. Devlin B, Roeder K (1999) Genomic control for association studies. *Biometrics* 55: 997-
718 1004.
- 719 7. Elshire RJ, Glaubitz JC, Sun Q, Poland JA, Kawamoto K, Buckler ES, Mitchell SE (2011) A
720 robust, simple genotyping-by-sequencing (GBS) approach for high diversity species. *PLoS*
721 *One* 6: e19379.

- 722 8. Endelman JB (2011) Ridge regression and other kernels for genomic selection with R
723 package rrBLUP. *Plant Genome* 4: doi.org/10.3835/plantgenome2011.08.0024.
- 724 9. Falconer DS, Mackay TFC (1996) *Introduction to quantitative genetics*. Prentice Hall, Essex,
725 England.
- 726 10. Fradgley N, Gardner KA, Cockram J, Elderfield J, Hickey JM, Howell P, Jackson R, Mackay
727 IJ (2019) A large-scale pedigree resource of wheat reveals evidence for adaptation and
728 selection by breeders. *PLoS Biol* 17: e3000071.
- 729 11. Friedman J, Hastie T, Tibshirani R (2010) Regularization paths for generalized linear models
730 via coordinate descent. *J Stat Softw* 33: 1-22.
- 731 12. Gaynor RC, Gorjanc G, Hickey JM (2021) AlphaSimR: an R package for breeding program
732 simulations. *G3: Genes, Genomes, Genetics* 11: jkaa017.
- 733 13. Gill BS, Friebe BR, White FF (2011) Alien introgressions represent a rich source of genes
734 for crop improvement. *Proc Natl Acad Sci USA* 108: 7657-7658.
- 735 14. Gorjanc G, Jenko J, Hearne SJ, Hickey JM (2016) Initiating maize pre-breeding programs
736 using genomic selection to harness polygenic variation from landrace populations. *BMC*
737 *Genomics* 17: 30.
- 738 15. Gorroochurn P, Heiman GA, Hodge SE, Greenberg DA (2006) Centralizing the non-central
739 chi-square: a new method to correct for population stratification in genetic case-control
740 association studies. *Genet Epidemiol* 30: 277-289.
- 741 16. Griffiths S, Simmonds J, Leverington M, Wang Y, Fish L, Sayers L, Alibert L, Orford S,
742 Wingen L, Herry L, Faure S, Laurie D, Bilham L, Snape J (2010) Meta-QTL analysis of the
743 genetic control of crop height in elite European winter wheat germplasm. *Mol Breed* 29: 159-
744 171.
- 745 17. Haque MA, Martinek P, Watanabe N, Kuboyama T (2011) Genetic mapping of gibberellic
746 acid-sensitive genes for semi-dwarfism in durum wheat. *Cereal Res Commun* 39: 171-178.

- 747 18. Hickey JM, Chiurugwi T, Mackay I, Powell W, Implementing Genomic Selection in CGIAR
748 Breeding Programs Workshop Participants (2017) Genomic prediction unifies animal and
749 plant breeding programs to form platforms for biological discovery. *Nat Genet* 49: 1297-
750 1303.
- 751 19. Hoad SP (2010) Evaluation of new varieties for sustainable cereal production in Europe.
752 Farmers Club Charitable Trust. [https://pure.sruc.ac.uk/en/publications/e0ac4808-c755-4f70-](https://pure.sruc.ac.uk/en/publications/e0ac4808-c755-4f70-a224-4bc536106813)
753 [a224-4bc536106813](https://pure.sruc.ac.uk/en/publications/e0ac4808-c755-4f70-a224-4bc536106813). Accessed 25 November 2021.
- 754 20. Hoerl AE, Kennard RW (1970) Ridge regression: biased estimation for nonorthogonal
755 problems. *Technometrics* 12: 55-67.
- 756 21. Jiang W, Zhang X, Li S, Song S, Zhao H (2021) Correcting statistical bias in correlation-
757 based kinship estimators. *Biorxiv*. doi.org/10.1101/2021.01.13.426515
- 758 22. Johnsson M (2018) Integrating selection mapping with genetic mapping and functional
759 genomics. *Front Genet* 9: 603.
- 760 23. Johnsson M, Gaynor RC, Jenko J, Gorjanc G, de Koning DJ, Hickey JM (2019) Removal of
761 alleles by genome editing (RAGE) against deleterious load. *Genet Sel Evol* 51: 14.
- 762 24. Ladejobi O, Mackay IJ, Poland J, Praud S, Hibberd JM, Bentley AR (2019) Reference
763 genome anchoring of high-density markers for association mapping and genomic prediction
764 in European winter wheat. *Front Plant Sci* 10: 1278.
- 765 25. Lande R, Arnold SJ (1983) The measurement of selection on correlated characters.
766 *Evolution* 37: 1210-1226.
- 767 26. Li J, Chen G-B, Rasheed A, Li D, Sonder K, Espinosas CZ, Wang JK, Costich DE, Schnable
768 PS, Hearne SJ, Li H (2020) Identifying loci with breeding potential across temperate and
769 tropical adaptation via EigenGWAS and EnvGWAS. *Mol Ecol* 28: 3544-3560.
- 770 27. Looseley ME, Ramsay L, Bull H, Swanston JS, Shaw PD, Macaulay M, Booth A, Russell JR,
771 Waugh R, Thomas WTB (2020) Association mapping of malting quality traits in UK spring
772 and winter barley cultivar collections. *Theor Appl Genet* 133: 2567-2582.

- 773 28. Mackay I, Horwell A, Garner J, White J, McKee J, Philpott H (2011) Reanalyses of the
774 historical series of UK variety trials to quantify the contributions of genetic and
775 environmental factors to trends and variability in yield over time. *Theor Appl Genet* 122: 225-
776 238.
- 777 29. Marchal C, Zhang J, Zhang P, Fenwick P, Steuernagel B, Adamski NM, Boyd L, McIntosh R,
778 Wulff BBH, Berry S, Lagudah E, Uauy C (2018) BED-domain-containing immune receptors
779 confer diverse resistance spectra to yellow rust. *Nat Plants* 4: 662-668.
- 780 30. Martynov SP, Dobrotvorskaya TV, Krupnov VA (2018) Analysis of the distribution of *Triticum*
781 *timopheevii* Zhuk. Genetic material in common wheat varieties (*Triticum aestivum* L.). *Russ*
782 *J Genet* 54: 166-175.
- 783 31. Meuwissen TH, Hayes BJ, Goddard ME (2001) Prediction of total genetic value using
784 genome-wide dense marker maps. *Genetics* 157: 1819-1829.
- 785 32. Mo Y, Vanzetti LS, Hale I, Spagnolo EJ, Guidobaldi F, Al-Oboudi J, Odle N, Pearce S,
786 Helguera M, Dubcovsky J (2018) Identification and characterization of *Rht25*, a locus on
787 chromosome arm 6AS affecting wheat plant height, heading time, and spike development.
788 *Theor Appl Genet* 131: 2021-2035.
- 789 33. Mohler V, Lukman R, Ortiz-Islas S, William M, Worland AJ, van Beem J, Wenzel G (2004)
790 Genetic and physical mapping of photoperiod insensitive gene *Ppd-B1* in common wheat.
791 *Euphytica* 138: 33-40.
- 792 34. Ochoa A, Storey JD (2021) Estimating F_{ST} and kinship for arbitrary population structures.
793 *PLoS Genet.* 17: e1009241.
- 794 35. Pearce S, Saville R, Vaughan SP, Chandler PM, Wilhelm EP, Sparks CA, Al-Kaff N, Korolev
795 A, Boulton MI, Phillips AL, Hedden P, Nicholson P, Thomas SG (2011) Molecular
796 characterization of *Rht-1* dwarfing genes in hexaploid wheat. *Plant Physiol* 157: 1820-1831.
- 797 36. Prentice RL, Pyke R (1979) Logistic disease incidence models and case-control studies.
798 *Biometrika* 66: 403-411.

- 799 37. R Core Team (2021) R: A language and environment for statistical computing. R Foundation
800 for Statistical Computing, Vienna.
- 801 38. Reif JC, Zhang P, Dreisigacker S, Warburton ML, van Ginkel M, Hoisington D, Bohn M,
802 Melchinger AE (2005) Wheat genetic diversity trends during domestication and breeding.
803 *Theor Appl Genet* 110: 859-864.
- 804 39. Rhoné B, Raquin AL, Goldringer I (2007) Strong linkage disequilibrium near the selected
805 *Yr17* resistance gene in a wheat experimental population. *Theor Appl Genet* 114: 787-802.
- 806 40. Robert O, Abelard C, Dedryver F (1999) Identification of molecular markers for the detection
807 of the yellow rust resistance gene *Yr17* in wheat. *Mol Breed* 5: 167-175.
- 808 41. Rosyara UR, de Jong WS, Douches DS, Endelman JB (2016) Software for genome-wide
809 association studies in autopolyploids and its application to potato. *Plant Genome* 9: 1-10.
- 810 42. Rowan TN, Durbin HJ, Seabury CM, Schnabel RD, Decker JE (2021) Powerful detection of
811 polygenic selection and evidence of environmental adaptation in US beef cattle. *PLoS*
812 *Genet* 17: e1009652.
- 813 43. Santantonio N, Jannink J-L, Sorrells M (2019) A low resolution epistasis mapping approach
814 to identify chromosome arm interactions in allohexaploid wheat. *G3: Genes, Genomes,*
815 *Genetics* 9: 675-684.
- 816 44. Schork NJ (2001) Genome partitioning and whole-genome analysis. *Adv Genet* 42: 299-
817 322.
- 818 45. Scott MF, Fradgley N, Bentley AR, Brabbs T, Corke F, Gardner KA, Horsnell R, Howell P,
819 Ladejobi O, Mackay IJ, Mott R, Cockram J (2021) Limited haplotype diversity underlies
820 polygenic trait architecture across 70 years of wheat breeding. *Genome Biol* 22: 137.
- 821 46. Sharma R, Cockram J, Gardner KA, Russell J, Ramsay L, Thomas WTB, O'Sullivan DM,
822 Powell W, Mackay IJ (2021) Trends of genetic changes uncovered by Env- and Eigen-
823 GWAS in wheat and barley. *Theor Appl Genet*. doi.org/10.1007/s00122-021-03991-z

- 824 47. Shorinola O, Simmonds J, Wingen LU, Gardner K, Uauy C (2021) Trend, population
825 structure and trait mapping from 15 years of national varietal trials of UK winter wheat.
826 *Biorxiv*. doi.org/10.1101/2021.05.17.444481
- 827 48. Singh S, Jighly A, Sehgal D, Burgueño J, Joukhadar R, Singh SK, Sharma A, Vikram P,
828 Sansaloni CP, Govindan V, Bhavani S, Randhawa M, Solis-Moya E, Singh S, Pardo N, Arif
829 MAR, Laghari KA, Basandrai D, Shokat S, Chaudhary HK, Saeed NA, Basandrai AK,
830 Ledesma-Ramírez L, Sohu VS, Imtiaz M, Sial MA, Wenzl P, Singh GP, Bains NS (2021)
831 Direct introgression of untapped diversity into elite wheat lines. *Nat Food* 2: 819-827.
- 832 49. Su Z, Hao C, Wang L, Dong Y, Zhang X (2011) Identification and development of a
833 functional marker of *TaGW2* associated with grain weight in bread wheat (*Triticum aestivum*
834 L.) *Theor Appl Genet* 122: 211-223.
- 835 50. Tadesse W, Sanchez-Garcia M, Assefa SG, Amri A, Bishaw Z, Ogonnaya FC, Baum M
836 (2019) Genetic gains in wheat breeding and its role in feeding the world. *Crop Breed Genet*
837 *Genom* 1: e190005.
- 838 51. Tibshirani R (1996) Regression shrinkage and selection via the lasso. *J R Stat Soc* 58: 267-
839 288.
- 840 52. Tiwari C, Wallwork H, Arun B, Mishra VK, Velu G, Stangoulis J, Kumar U, Joshi AK (2016)
841 Molecular mapping of quantitative trait loci for zinc, iron and protein content in the grains of
842 hexaploidy wheat. *Euphytica* 207: 563-570.
- 843 53. Tsilo TJ, Jin Y, Anderson JA (2008) Diagnostic microsatellite markers for the detection of
844 stem rust resistance gene *Sr36* in diverse genetic backgrounds of wheat. *Crop Sci* 48: 253-
845 261.
- 846 54. Visscher PM, Macgregor S, Benyamin B, Zhu G, Gordon S, Medland S, Hill WG, Hottenga
847 J-J, Willemsen G, Boomsma DI, Liu Y-Z, Deng H-W, Montgomery GW, Martin NG (2007)
848 Genome partitioning of genetic variation for height from 11,214 sibling pairs. *Am J Hum*
849 *Genet* 81: 1104-1110.

- 850 55. Voss-Fels KP, Cooper M, Hayes BJ (2018) Accelerating crop genetic gains with genomic
851 selection. *Theor Appl Genet* 132: 669-686.
- 852 56. Walsh B, Lynch M. Evolution and selection of quantitative traits. Oxford University Press,
853 Oxford (2018).
- 854 57. Wang S, Wong D, Forrest K, Allen A, Chao S, Huang BE, Maccaferri M, Salvi S, Milner SG,
855 Cattivelli L, Mastrangelo AM, Whan A, Stephen S, Barker G, Wieseke R, Plieske J, IWGSC,
856 Lillemo M, Mather D, Appels R, Dolferus R, Brown-Guedira G, Korol A, Akhunova AR,
857 Feuillet C, Salse J, Morgante M, Pozniak C, Luo M-C, Dvorak J, Morrell M, Dubcovsky J,
858 Ganal M, Tuberosa R, Lawley C, Mikoulitch I, Cavanagh C, Edwards KJ, Hayden M,
859 Akhunov E (2014) Characterization of polyploid wheat genomic diversity using a high-
860 density 90,000 single nucleotide polymorphism array. *Plant Biotechnol J* 12: 787-796.
- 861 58. Würschum T, Langer SM, Longin CFH, Tucker MR, Leiser WL (2017) A modern Green
862 Revolution gene for reduced height in wheat. *Plant J* 92: 892-903.
- 863 59. Yang CJ, Sharma R, Gorjanc G, Hearne S, Powell W, Mackay I (2020) Origin specific
864 genomic selection: a simple process to optimize the favorable contribution of parents to
865 progeny. *G3: Genes, Genomes, Genetics* 10: 2445-2455.
- 866 60. Yang Y, Aduragbemi A, Wei D, Chai Y, Zheng J, Qiao P, Cui C, Lu S, Chen L, Hu Y-G
867 (2021) Large-scale integration of meta-QTL and genome-wide association study discovers
868 the genomic regions and candidate genes for yield and yield-related traits in bread wheat.
869 Research Square. doi.org/10.21203/rs.3.rs-342038/v1
- 870 61. Yu J, Pressoir G, Briggs WH, Bi IV, Yamasaki M, Doebley JF, McMullen MD, Gaut BS,
871 Nielsen DM, Holland JB, Kresovich S, Buckler ES (2006) A unified mixed-model method for
872 association mapping that accounts for multiple levels of relatedness. *Nat Genet* 38: 203-
873 208.

874 **Tables and Figures**

875 **Table 1. Genomic positions of 22 RALLY QSLs in the TG panel.**

876 The IWGSC RefSeq v1.0 physical positions of the peaks and LD boundaries are shown, along
 877 with the $-\log_{10}P$ scores associated with the peaks and overlapping QSLs/QTLs from RALLY in
 878 WAGTAIL panel and GWAS in TG panel (Ladejobi et al. 2019).

QSL	Chr	Position (bp)			$-\log_{10}P$	Overlapping QSLs/QTLs	
		Peak	Start	End		WAGTAIL	GWAS
1	1A	40,535,368	36,797,100	42,151,448	6.964	2	1
2	1A	138,028,803	105,888,613	395,485,807	6.419	2	0
3	1B	274,240,580	52,771,404	572,972,254	8.726	3	0
4	2A	19,049,803	502,328	36,134,675	7.022	5	7
5	2A	56,159,824	56,159,824	115,431,692	7.951	6	0
6	2B	230,348,363	10,888,962	785,614,875	10.634	9,10	10
7	3A	544,972,180	488,305,885	574,586,196	6.965	13	19
8	3B	20,035,143	19,086,765	31,366,713	6.011	0	0
9	3B	829,382,536	813,333,316	829,954,621	9.170	0	0
10	4A	690,425,855	507,739,498	695,893,542	7.199	14	22
11	4B	570,537,081	507,170,910	593,797,914	5.934	0	26,27
12	5A	59,666,472	31,088,127	449,788,941	7.816	16	28
13	5B	703,651,326	681,349,598	703,858,824	5.923	0	0
14	5D	69,776,655	43,408,942	233,674,405	6.148	0	0
15	6A	2,160,664	684,328	5,113,555	7.259	0	32
16	6A	89,355,276	61,817,777	545,399,189	6.538	18	33 - 37
17	6A	609,106,971	596,590,923	617,255,792	6.468	0	38
18	7A	612,599,663	610,209,166	612,599,663	6.272	0	0
19	7A	681,696,004	669,820,116	695,003,193	6.632	0	0
20	7B	3,693,110	3,366,069	4,826,131	6.438	0	0
21	7B	43,221,041	40,293,564	58,886,832	6.503	0	48
22	7B	704,838,082	698,229,993	707,941,517	7.952	0	49

879

880

881 **Table 2. Local heritabilities associated with 22 RALLY QSLs.**

882 Local heritabilities less than 0.001 are not shown.

QSL	FT	LODG	YLD	HT	PROT	WK	AWNS	SPWT	TGW	EM2	TILL	MAT
1	-	-	-	0.054	0.048	0.051	-	-	-	0.005	-	-
2	-	-	0.007	0.068	0.105	-	-	-	0.003	0.043	-	-
3	0.084	-	0.006	-	0.014	-	-	-	-	0.002	0.000	0.060
4	-	-	-	-	-	-	0.001	-	-	-	0.016	-
5	-	0.009	-	0.002	-	-	-	-	-	-	-	-
6	-	-	0.009	-	-	0.003	-	-	0.009	-	-	0.037
7	-	-	-	-	-	-	0.014	-	0.055	-	0.009	-
8	0.005	-	-	-	-	-	-	0.020	-	-	-	-
9	-	-	-	-	0.002	-	0.004	-	-	-	0.006	-
10	0.010	0.000	-	-	-	0.002	0.003	0.008	0.090	-	0.012	0.019
11	-	0.040	0.036	-	0.012	0.002	0.011	0.005	0.005	-	-	-
12	-	-	0.003	-	-	0.005	0.011	0.075	-	0.003	-	-
13	-	-	0.006	-	-	0.049	-	-	0.002	-	-	-
14	0.069	-	0.019	-	0.018	0.000	-	-	-	-	-	0.006
15	0.011	-	-	-	-	0.004	0.018	-	0.005	0.014	-	-
16	-	0.086	0.045	0.127	0.071	-	-	0.013	0.012	0.021	-	0.006
17	0.072	-	0.001	-	0.001	0.016	-	-	0.002	-	0.013	0.069
18	-	-	0.006	-	-	-	-	-	0.003	-	-	-
19	-	0.020	0.005	-	-	-	0.011	-	0.028	0.001	-	-
20	-	-	0.008	0.089	0.004	0.000	-	-	-	0.065	-	-
21	-	0.039	-	0.041	-	-	-	0.009	0.025	-	-	-
22	0.010	-	0.001	0.021	-	-	-	-	0.016	-	0.013	-
Total	0.260	0.194	0.153	0.402	0.275	0.133	0.074	0.129	0.254	0.154	0.068	0.197
Others	0.284	0.123	0.160	0.223	0.205	0.220	0.583	0.156	0.050	0.216	0.051	0.179

883

884 **Table 3. Counts of pairwise LASSO effects for alleles that are increasing over time.**

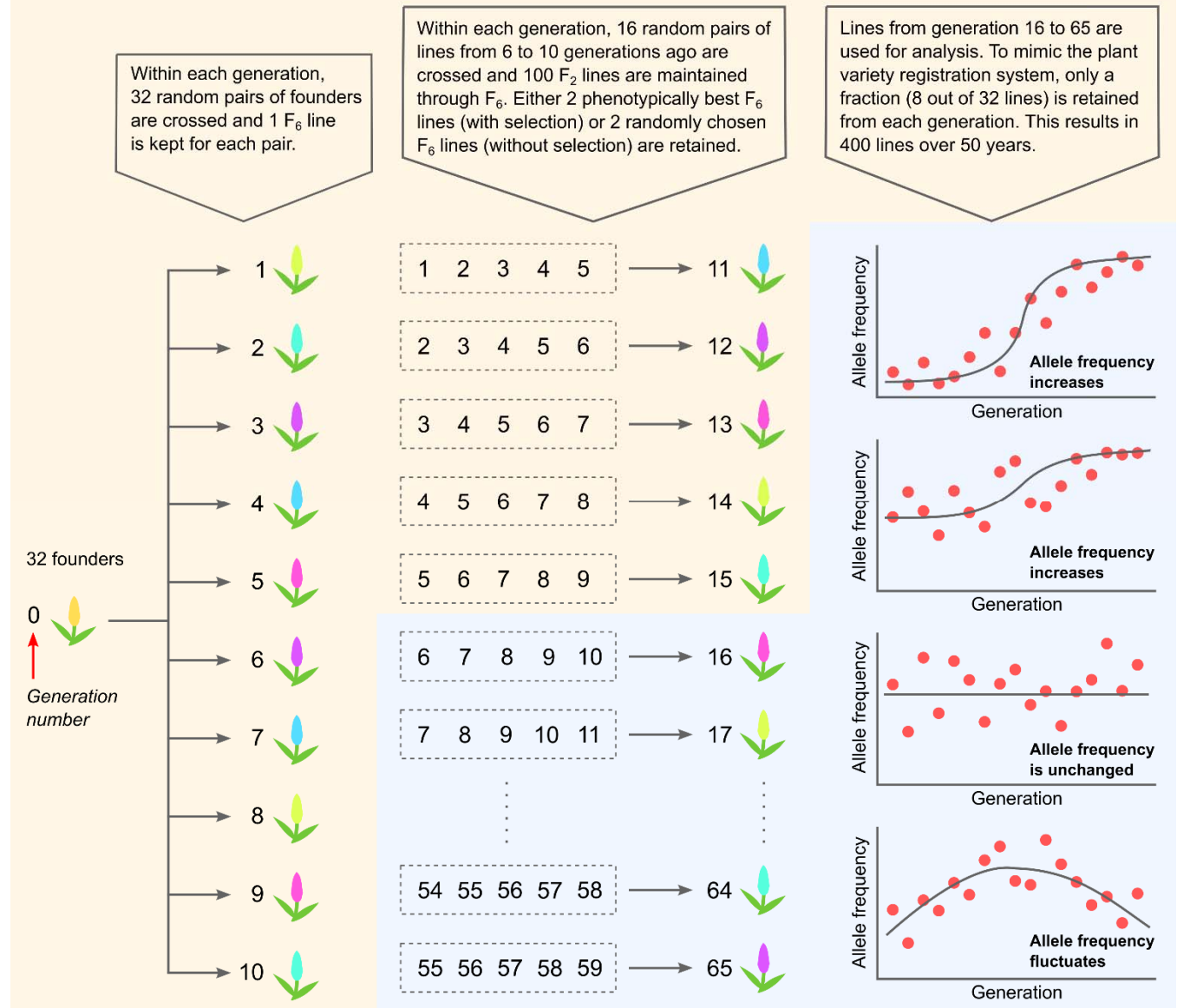
885 For each allele with increasing frequency over time, it is classified into pairs of traits for which
886 the allele has an increasing effect on both traits (+/+), a decreasing effect on both traits (-/-) or
887 antagonistic effects (+/- and -/+). The distribution for each pair of traits is tested with a $\chi^2_{df=1}$
888 contingency table where the significant threshold is set to $-\log_{10}p = 3.121$ (equivalent to a
889 Bonferroni-corrected threshold of $p = 0.05$ for 66 possible pairs of traits). Only the significant
890 trait pairs are shown here, and the full results are available in Table S7.

trait pair	+/+	+/-	-/+	-/-	$-\log_{10}p$
FT/YLD	270	43	145	59	4.435
FT/HT	112	201	22	182	9.352
FT/WK	135	178	135	69	6.326
FT/AWNS	139	174	140	64	6.959
FT/MAT	268	45	57	147	38.908
LODG/HT	75	56	59	327	20.083
YLD/PROT	74	341	62	40	17.486
YLD/MAT	280	135	45	57	4.687
HT/PROT	56	78	80	303	5.408
HT/WK	34	100	236	147	11.996
HT/AWNS	49	85	230	153	5.361
HT/MAT	102	32	223	160	3.474
PROT/SPWT	82	54	138	243	5.742
AWNS/MAT	145	134	180	58	7.317
SPWT/EM2	148	72	122	175	8.195
SPWT/MAT	119	101	206	91	3.269
TGW/EM2	85	131	185	116	5.962
EM2/MAT	149	121	176	71	3.643

891

892

893

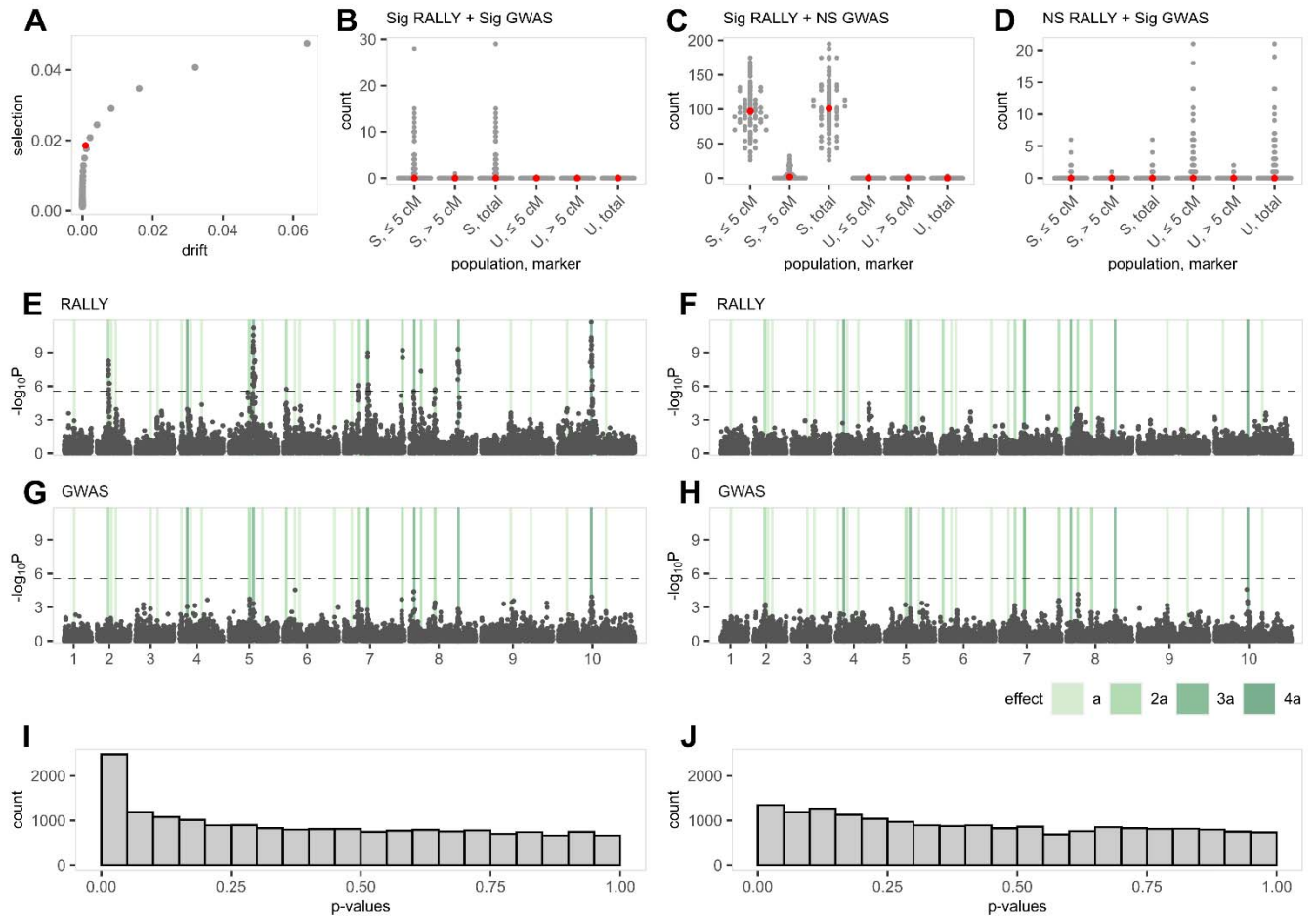


894

895 **Figure 1. Population simulation and changes in allele frequency over time.**

896 The simulated populations with and without selection are described in detail here. The first 15
 897 generations were used as burn-ins and discarded. 8 varieties from each generation starting at
 898 16 and ending at 65 were randomly chosen to create a population of 400 varieties that span
 899 over 50 generations. Examples of how allele frequency changes over time are shown, with the
 900 first two examples follows a logistic distribution and thus are more likely to be significant under
 901 RALLY than the other two examples.

902



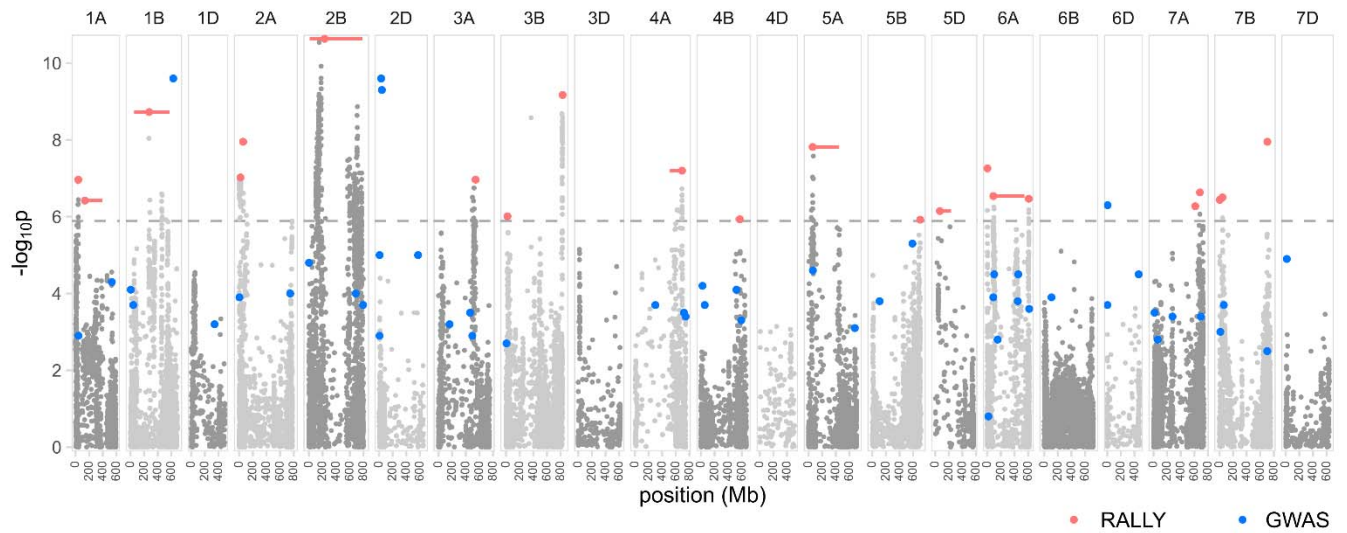
903

904 **Figure 2. RALLY and GWAS in simulated populations.**

905 Selected (S) and unselected (U) populations are simulated for 100 times and mapped for
 906 QSLs/QTLs using RALLY and GWAS. **[A]** Significant proportions of total markers identified from
 907 RALLY in S and U populations are calculated under various thresholds used in choosing null
 908 markers for delta control (DC) and genomic control (GC). The red point is estimated without DC
 909 and GC (uncorrected). Under the assumption that significant markers in U are due to drift alone
 910 and in S are due to both drift and selection, the X-axis is shown as the proportions in U while the
 911 Y-axis is shown as the differences in proportions between S and U. **[B – D]** Counts of significant
 912 markers identified from RALLY and GWAS are shown according to their distance from QTLs in
 913 both S and U populations. Medians are shown in red points. **[E]** Manhattan plot for RALLY in
 914 one simulated S population. QTLs are highlighted in vertical bars according to their effect sizes.
 915 **[F]** Manhattan plot for RALLY in one simulated U population. **[G]** Manhattan plot for GWAS in
 916 one simulated S population. **[H]** Manhattan plot for GWAS in one simulated U population. **[I]**
 917 Histogram of RALLY p-values for the same simulated S population. **[J]** Histogram of RALLY p-
 918 values in the same simulated U population.

919

920



921

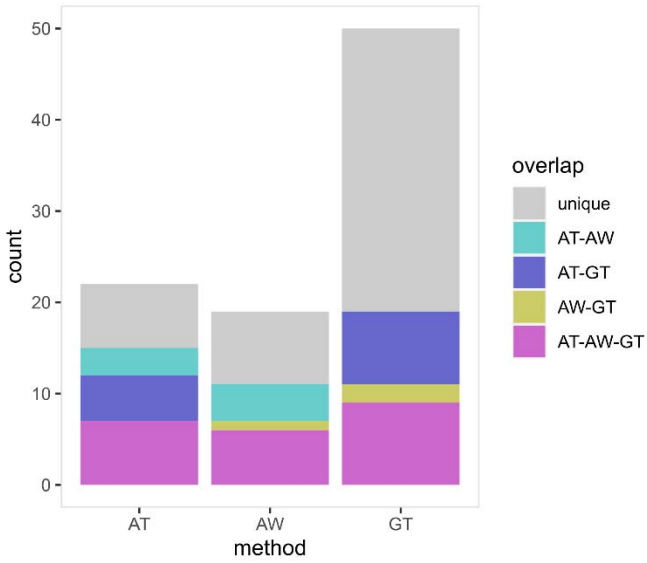
922 **Figure 3. Manhattan plot for RALLY results in the TG panel.**

923 RALLY peaks and their extents of LD are shown in red points and horizontal bars, respectively.

924 GWAS peaks from Ladejobi et al. (2019) are shown in blue points. The dashed horizontal line

925 represents the Bonferroni threshold of 0.05.

926

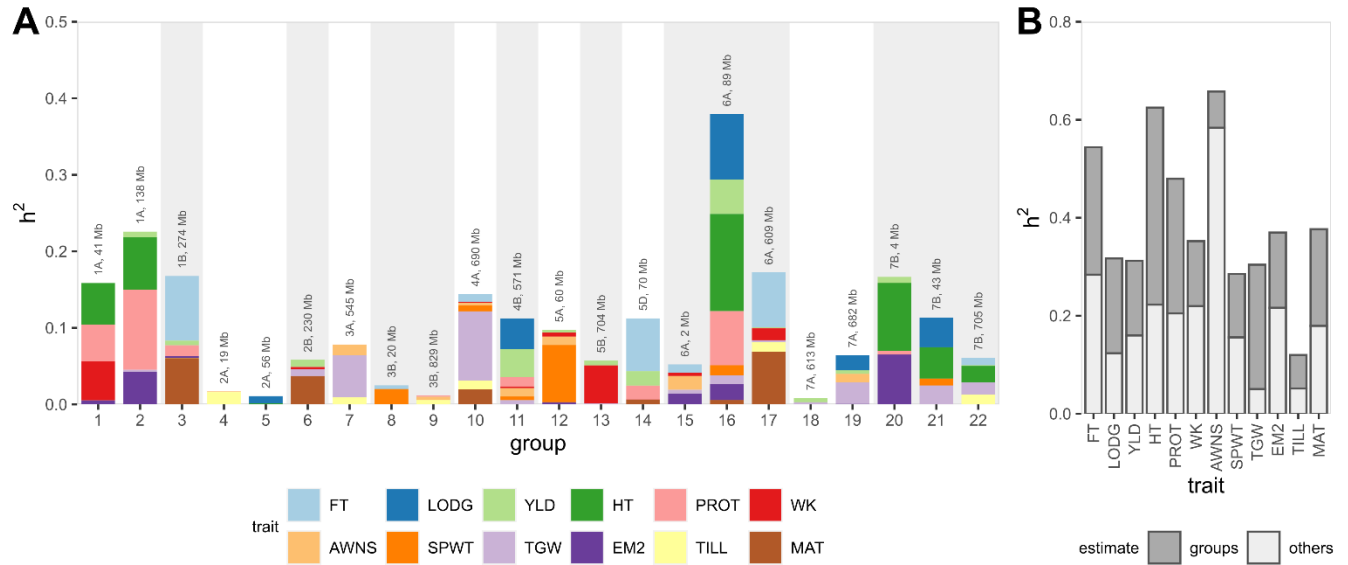


927

928 **Figure 4. QSL/QTL overlaps across different results.**

929 The number of overlapping QTLs among RALLY in TG panel (AT), RALLY in WAGTAIL panel
930 (AW) and GWAS in TG panel (GT) are shown.

931



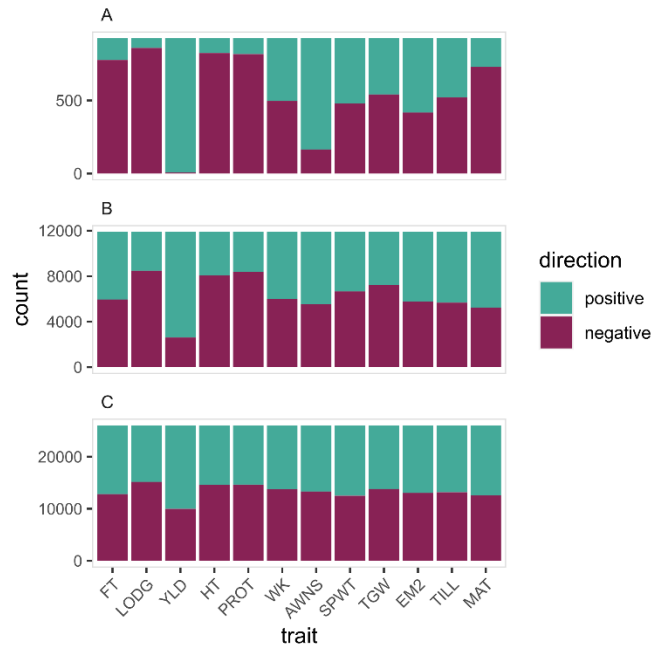
932

933 **Figure 5. Local heritabilities in RALLY QSL groups.**

934 **[A]** Local heritabilities for all 12 traits are shown as stacked bars for each RALLY QSL (defined
 935 in [Table 1](#)). **[B]** Local heritabilities from 22 RALLY groups are summed and compared against
 936 the heritabilities from other genomic markers.

937

938

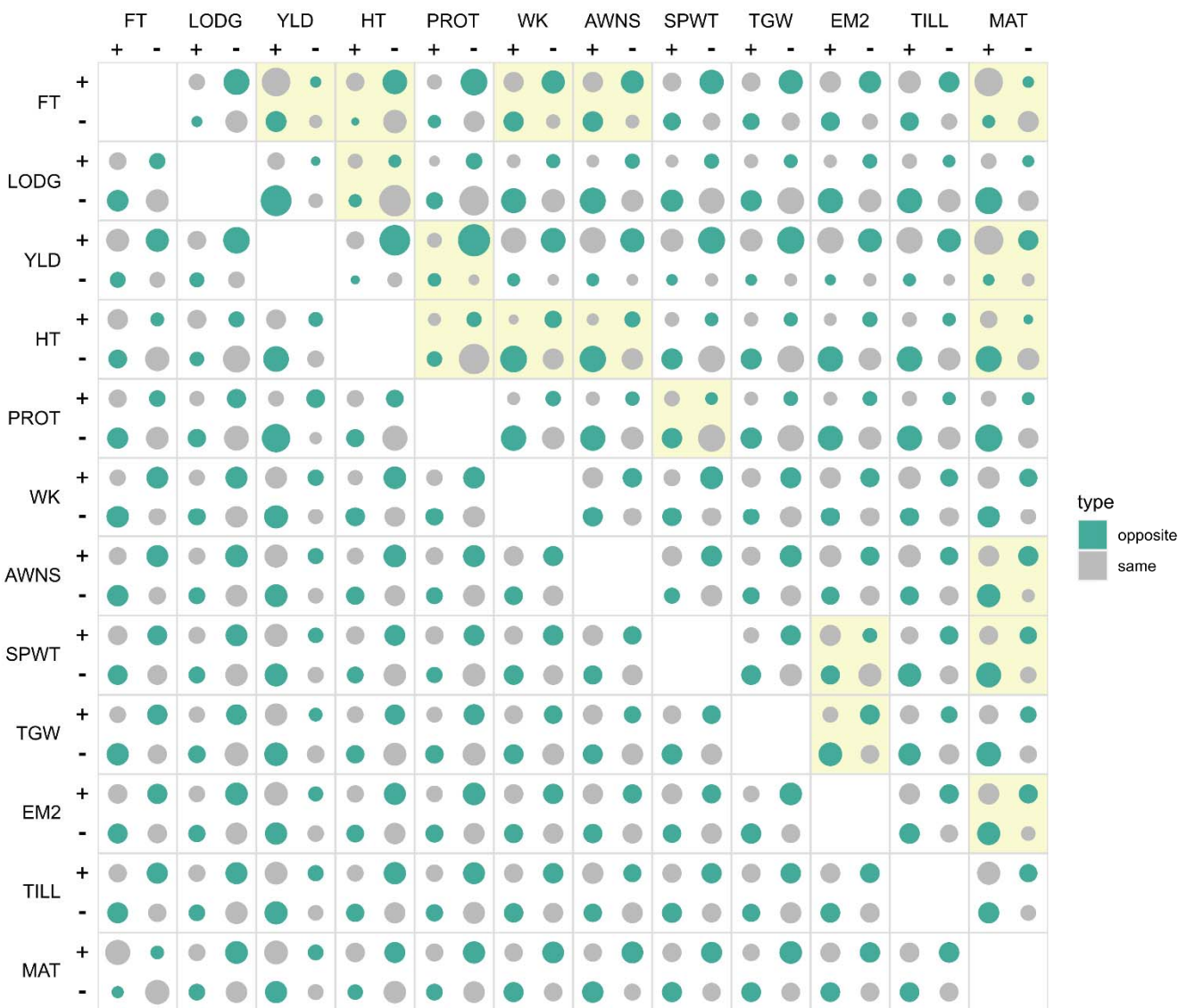


939

940 **Figure 6. Distributions of positive and negative RR effects in the increasing alleles.**

941 [A] Markers with RALLY P-values of lower than the Bonferroni corrected threshold. [B] Markers
942 with RALLY P-values between 0.05 and the Bonferroni corrected threshold. [C] Markers with
943 RALLY P-values of higher than 0.05.

944



945

946 **Figure 7. Distribution of pairwise effects for alleles with increasing frequency over time.**

947 For each allele with increasing frequency over time, it is classified into pairs of traits for which
 948 the allele has an increasing effect on both traits (+/+), a decreasing effect on both traits (-/-) or
 949 antagonistic/opposite effects (+/- and -/+). The circle areas are scaled according to the marker
 950 counts. The bottom left triangle represents the RR effects and the top right triangle represents
 951 the LASSO effects. The distributions of the effect classes in each trait pair are tested using
 952 in the LASSO effects and significant results (Bonferroni-corrected threshold of $p = 0.05$)
 953 are highlighted in yellow. No test is performed in the RR effects because the marker effects in
 954 RR are not independent.

955

956

957